J Mater Sci: Mater Electron (2016) 27:2589–2593
DOI 10.1007/s10854-015-4062-4

Green synthesis and characterization of lead titanate nanoparticles and its photocatalyst application

Sogol Shabanalizadeh[1] · Ali Abedini[2] · Amin Alborzi[2] · Mahvash Bahmani[3] · Naghmeh Shaghaghi[4] · Sasan Hajebi[5] · Matin Yazdanmehr[5]

Received: 17 August 2015 / Accepted: 8 November 2015 / Published online: 17 November 2015

Abstract Pure lead titanate ($PbTiO_3$) nanoparticles were successfully synthesized by novel sol–gel method with the aid of $Pb(CH_3COO)_2{\cdot}3H_2O$, $Ti(OC_4H_9)_4$ (TNBT), and glucose without adding external surfactant. Moreover, glucose plays role as reducing agent, and natural template in the synthesis $PbTiO_3$ nanoparticles. The structural, morphological and optical properties of as obtained products were characterized by techniques such X-ray diffraction, energy dispersive X-ray microanalysis, scanning electron microscopy, and ultraviolet–visible spectroscopy. To evaluate the photocatalyst properties of nanocrystalline lead titanate, the photocatalytic degradation of methyl orange under ultraviolet light irradiation was carried out.

1 Introduction

Physical properties and potential applications of nanostructures and nanomaterial have been studied intensively [1–3]. This interest results from the special properties of materials at the nanoscale, such as a large surface-to-volume ratio and increased surface activity, as compared with that of the bulk material. The properties of bulk materials usually depend on the size of the primary particles. Thus, the control of particle size and morphology plays a crucial role in the manufacturing process [4–8]. $PbTiO_3$ (PT) with tetragonal perovskite structure at room temperature is a ferroelectric compound with Curie temperature of 490 °C, high pyroelectric coefficient, high spontaneous polarization, and low dielectric constant [9]. PT is widely applied in electronics such as multilayer capacitor, resonators, and ultrasonic transducers due to a large pyroelectric coefficient and a relatively low permittivity. The crystalline structure of PT was determined by neutron diffraction and presented tetragonal symmetry [10–14]. Lead titanate when combined with other oxides can form a series of solid solution materials such as Pb(Zr, Ti)O_3(PZT) and (Pb, La)(Zr, Ti)O_3(PLZT), with potential applications in sensors, capacitors and non-volatile memories. Some authors have investigated PT materials modified by various additives [15, 16]. Lead titanate (PT) ceramics modified by rare earth elements and alkaline earth elements are extremely good for high frequency applications [17, 18]. The properties of these ceramics are strongly related to stoichiometry. The presences of intermediate phases can significantly damage the electrical properties [19]. The formation of lead deficient phases delay and even hinder the formation of perovskite [20]. Sirera and Calzada [21], upon obtaining pure and doped PT powders, observed the emergence of a pyrochlore phase which disappeared with the increase of the treatment temperature. Several methods have been used to obtain lead titanate powders, such as high-energy milling, sol–gel method, co-precipitation and hydrothermal synthesis, besides the traditional solid state reaction of mixed oxides [22–27]. In this report, for the first time, we

✉ Ali Abedini
aliabedini074@gmail.com

[1] Active Pharmaceutical Ingredients Research Center, Pharmaceutical Sciences Branch, Islamic Azad University, Tehran, Iran

[2] Young Researchers and Elite Club, Borujerd Branch, Islamic Azad University, Borujerd, Iran

[3] Tehran Medical Sciences Branch, Islamic Azad University, Tehran, Iran

[4] School of Nursing and Midwifery, Islamic Azad University, Tehran, Iran

[5] Faculty of Basic Science, Islamic Azad University, Borujerd, Iran

had presented the preparation of $PbTiO_3$ nanoparticles by novel sol–gel method at 700 °C in the presence of glucose without adding external surfactant, capping agent or template. A green approach for $PbTiO_3$ nanoparticles synthesis by utilizing natural template permits the reaction to proceed usually in milder conditions. Although existing chemical approaches have effectively produced well-defined $PbTiO_3$ nanoparticles, these processes are generally costly and include the employ of toxic chemicals. The photocatalytic degradation was investigated using methyl orange (MO) ultraviolet light irradiation [3, 28].

2 Experimental

2.1 Characterization

X-ray diffraction (XRD) patterns were recorded by a Philips-X'PertPro, X-ray diffractometer using Ni-filtered Cu Kα radiation at scan range of $10° < 2\theta < 80°$. Scanning electron microscopy (SEM) images were obtained on LEO-1455VP equipped with an energy dispersive X-ray spectroscopy. Spectroscopy analysis (UV–Vis) was carried out using shimadzu UV–Vis scanning UV–Vis diffuse reflectance spectrometer. The energy dispersive spectrometry (EDS) analysis was studied by XL30, Philips microscope.

2.2 Synthesis of $PbTiO_3$ nanoparticles

All the chemicals used in this method were of analytical grade and used as received without any further purification. At first, 1.1 g of lead (II) acetate, 1.1 g of glucose, and 0.5 ml acetylacetonate were dissolved in 10 ml distilled ethanol and stirred for 15 min. Then, 1 ml of tetra-*n*-butyl orthotitanate was added drop wise into solution. Afterwards, the final mixed solution was kept stirring to form a gel at 90 °C. Finally, the obtained product was placed in a conventional furnace in air atmosphere for 150 min and calcine at 700 °C. After thermal treatment, the system was allowed to cool to room temperature naturally, and the obtained precipitate was collected.

2.3 Photocatalysis experiments

The methyl orange (MO) photodegradation was examined as a model reaction to evaluate the photocatalytic activities of the lead titanate nanoparticles. The photocatalytic experiments were performed under an irradiation ultraviolet light. The photocatalytic activity of nanocrystalline lead titanate obtained was studied by the degradation of methyl orange solution as a target pollutant. The photocatalytic degradation was performed with 150 ml solution of methyl orange (0.0005 g) containing 0.1 g of $PbTiO_3$. This mixture was aerated for 30 min to reach adsorption equilibrium. Later, the mixture was placed inside the photoreactor in which the vessel was 15 cm away from the visible source of 400 W mercury lamps. The photocatalytic test was performed at room temperature. Aliquots of the mixture were taken at definite interval of times during the irradiation, and after centrifugation they were analyzed by a UV–Vis spectrometer. The methyl orange (MO) degradation percentage was calculated as:

$$\text{Degradation rate } (\%) = \frac{A_0 - A}{A_0} \times 100$$

where A_0 and A are the absorbance value of solution at A_0 and A min, respectively.

3 Results and discussion

Figure 1 shows a typical XRD pattern ($10° < 2\theta < 80°$) of $PbTiO_3$ nanoparticles. Based on the Fig. 1, the diffraction peaks can be indexed to pure tetragonal phase of $PbTiO_3$ (space group *P4/mmm*, JCPDS No. 75-0438). No other crystalline phases were detected. From XRD data, the crystallite diameter (D_c) of $PbTiO_3$ nanoparticles was calculated to be 40 nm using the Scherer equation:

$$D_c = K\lambda/\beta \cos\theta \qquad \text{(Scherer equation)}$$

where β is the breadth of the observed diffraction line at its half intensity maximum (400), K is the so-called shape factor, which usually takes a value of about 0.9, and λ is the wavelength of X-ray source used in XRD. The morphology of the nanoparticles was investigated using SEM which demonstrates uniform nanoparticles with spherical shape homogenously distributed all over the sample, as it could be clearly observed in Fig. 2. The $PbTiO_3$ nanoparticles with particle size of about 45–55 nm were observed. The EDS analysis measurement was used to investigate the chemical composition and purity of $PbTiO_3$ nanoparticles. According to the Fig. 3, the product consists of Pb, Ti, and O elements. Furthermore, neither N nor C signals were detected in the EDS spectrum, which means the product is pure and free of any surfactant or impurity. The room temperature UV–Vis absorption spectra of $PbTiO_3$ nanoparticles were also measured in the range of 300–600 nm. Figure 4 shows the diffuse reflection absorption spectra of the $PbTiO_3$ nanoparticles calcined at 700 °C. The figure indicates that the $PbTiO_3$ nanoparticles shows absorption maxima at 338 nm, the direct optical band gap estimated from the absorption spectra for the $PbTiO_3$ nanoparticles is shown in Fig. 5. An optical band gap is obtained by plotting $(\alpha h\nu)^2$ versus hν where α is the absorption coefficient and hν is photon energy. Extrapolation of the linear portion at $(\alpha h\nu)^2 = 0$ gives the band gaps of 2.8 eV for perovskite $PbTiO_3$ material. Photodegradation of

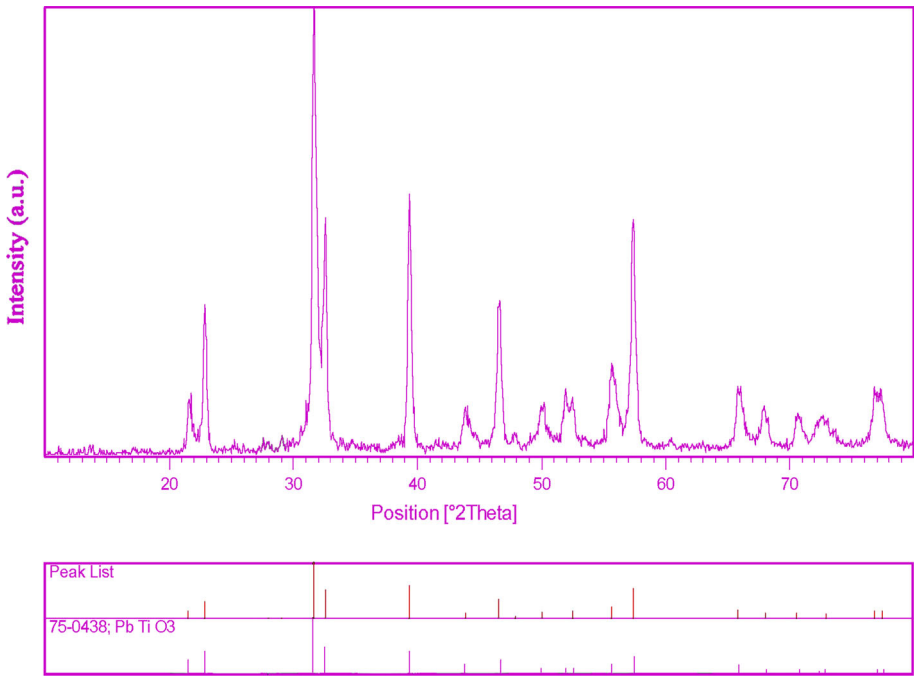

Fig. 1 XRD pattern of $PbTiO_3$ nanoparticles calcined at 700 °C

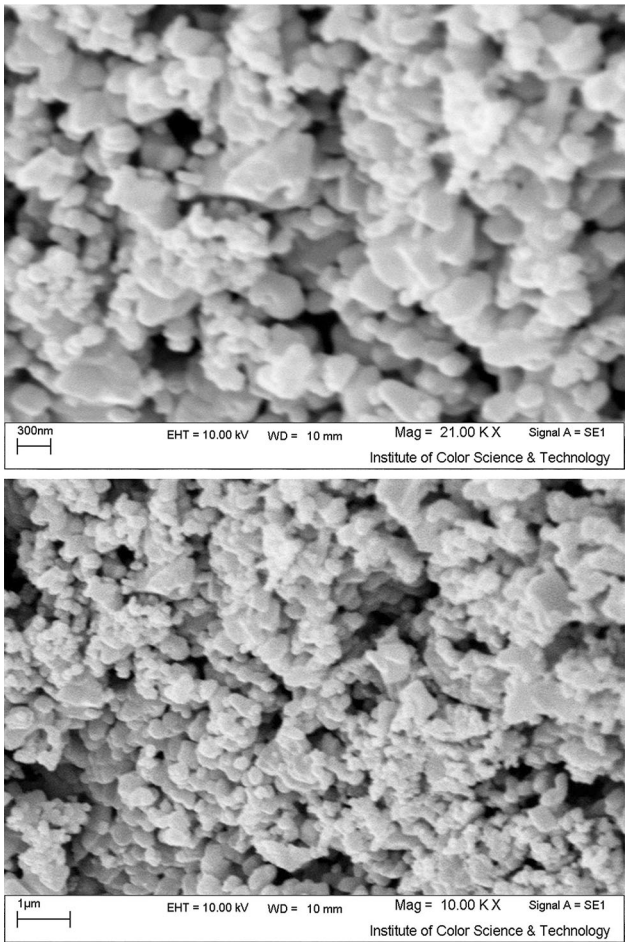

Fig. 2 SEM image of $PbTiO_3$ nanoparticles calcined at 700 °C

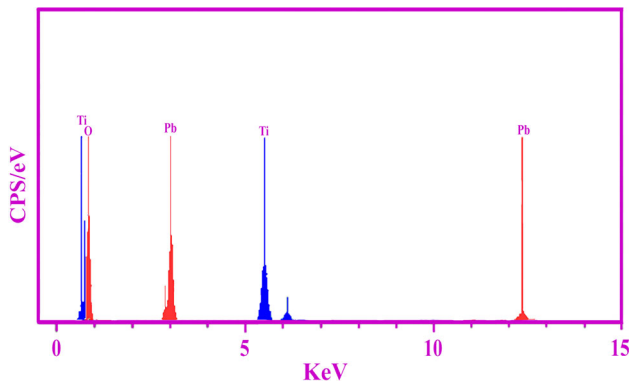

Fig. 3 EDS pattern of $PbTiO_3$ nanoparticles calcined at 700 °C

methyl orange under UV light irradiation (Fig. 6a–c) was employed to evaluate the photocatalytic activity of the as-synthesized $PbTiO_3$. No methyl orange was practically broken down after 60 min without using UV light irradiation or nanocrystalline $PbTiO_3$. This observation indicated that the contribution of self-degradation was insignificant. The probable mechanism of the photocatalytic degradation of methyl orange can be summarized as follows:

$$PbTiO_3 + h\nu \rightarrow PbTiO_3^{\cdot} + e^- + h^+ \quad (1)$$

$$h^+ + H_2O \rightarrow OH^{\cdot} \quad (2)$$

$$e^- + O_2 \rightarrow O_2^{\cdot -} \quad (3)$$

$$OH^{\cdot} + O_2^{\cdot -} + \text{methyl orange} \rightarrow \text{Degradation products} \quad (4)$$

Using photocatalytic calculations by Eq. (1), the methyl orange degradation was about 97 % after 60 min irradiation

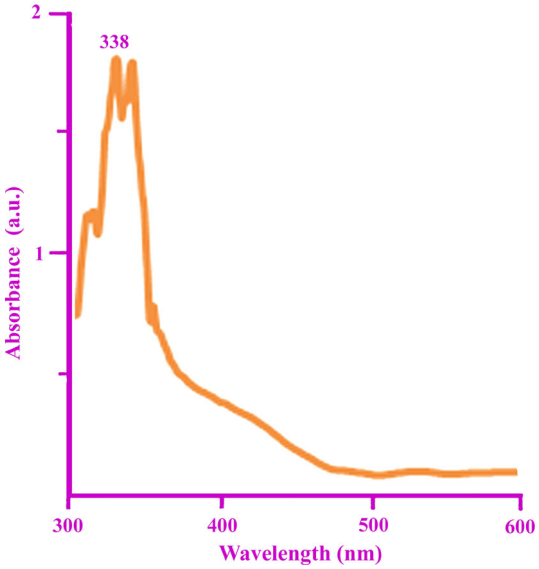

Fig. 4 UV–Vis absorption spectra of prepared $PbTiO_3$ nanoparticles for 150 min at calcination temperature of 700 °C

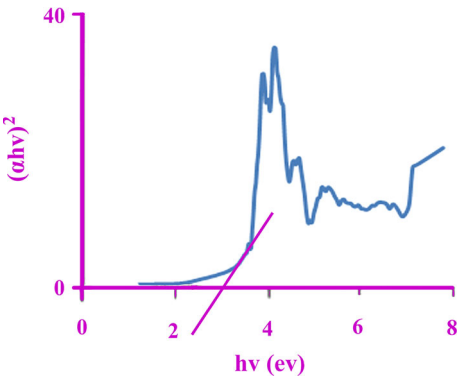

Fig. 5 Plot to determine the direct band gap of $PbTiO_3$

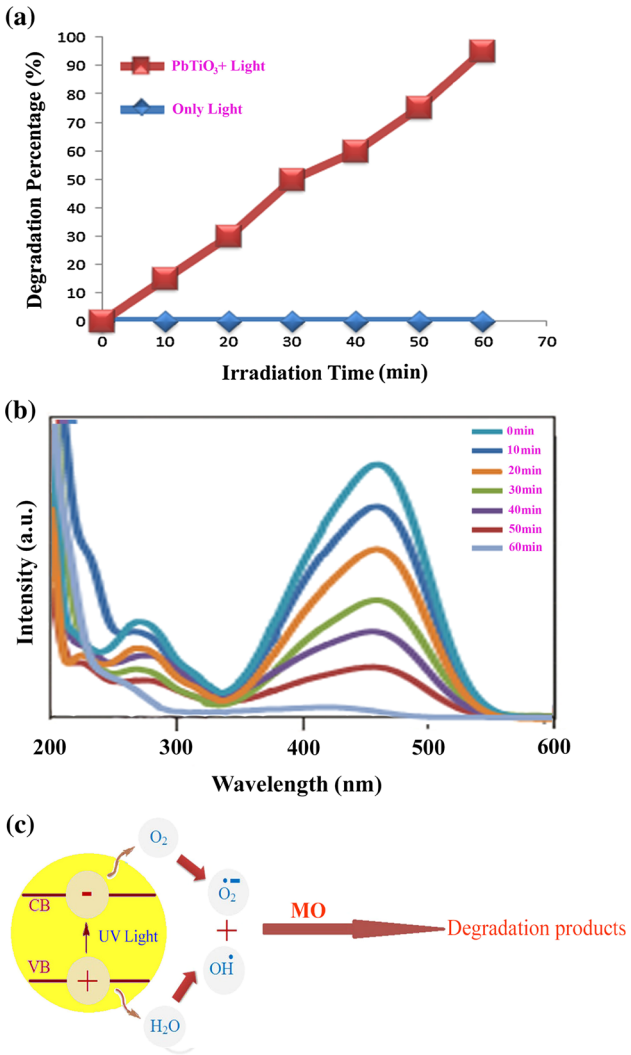

Fig. 6 **a** Photocatalytic methyl orange degradation of $PbTiO_3$ nanoparticles under ultraviolet light, **b** fluorescence spectral time scan of methyl orange illuminated at 510 nm with $PbTiO_3$ nanoparticles and **c** reaction mechanism of methyl orange photodegradation over $PbTiO_3$ nanoparticles under ultraviolet light irradiation

of UV light, and nanocrystalline $PbTiO_3$ presented high photocatalytic activity (Fig. 6a). The spectrofluorimetric time-scans of methyl orange solution illuminated at 510 nm with nanocrystalline $PbTiO_3$ are depicted in Fig. 6b. Figure 6b shows continuous removal of methyl orange on the $PbTiO_3$ under UV light irradiation. It is generally accepted that the heterogeneous photocatalytic processes comprise various steps (diffusion, adsorption, reaction, and etc.), and suitable distribution of the pore in the catalyst surface is effective and useful to diffusion of reactants and products, which prefer the photocatalytic reaction. In this investigation, the enhanced photocatalytic activity can be related to appropriate distribution of the pore in the nanocrystalline $PbTiO_3$ surface, high hydroxyl amount and high separation rate of charge carriers (Fig. 6c). Furthermore, this route is facile to operate and very suitable for industrial production of $PbTiO_3$ nanoparticles. In addition, this process can be versatile to easily synthesize other titanium based perovskite oxides. The synthesis pathway of $PbTiO_3$ nanoparticles is shown in Scheme 1.

4 Conclusions

In this work, lead titanate nanoparticles were successfully synthesized by a novel sol–gel method at 700 °C for 150 min. The stages of the formation of $PbTiO_3$, as well as the characterization of the resulting compounds were done using X-ray diffraction and energy dispersive X-ray spectroscopy. The products were analyzed by scanning electron microscopy (SEM), and ultraviolet–visible (UV–Vis) spectroscopy to be round, about 45–55 nm in size and

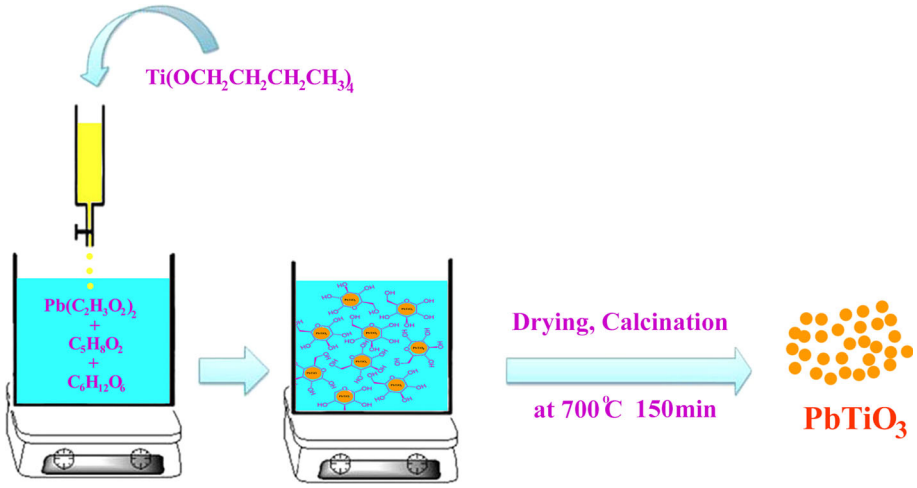

Scheme 1 Schematic diagram illustrating the formation of $PbTiO_3$ nanoparticles

Eg = 2.8 eV. When as-prepared nanocrystalline lead titanate oxide was utilized as photocatalyst, the percentage of methyl orange degradation was about 97 % after 60 min irradiation of UV light. This result suggests that as-obtained nanocrystalline lead titanate as favorable material has high potential to be used for photocatalytic applications under UV light.

Acknowledgments Authors are grateful to council of University of Borujerd for providing financial support to undertake this work.

Compliance with ethical standards

Conflict of interest The author declares that the research was conducted in the absence of any commercial or financial relationships that could be construed as a potential conflict of interest.

References

1. M. Najafi, H. Haratizadeh, M. Ghezellou, J. Nanostruct. **5**, 129 (2015)
2. S. Khademolhoseini, M. Zakeri, S. Rahnamaeiyan, M. Nasiri, R. Talebi, J. Mater. Sci. Mater. Electron. **26**, 7303 (2015)
3. F.S. Ghoreishi, V. Ahmadi, M. Samadpourc, J. Nanostruct. **3**, 453 (2013)
4. S. Moshtaghi, D. Ghanbari, M. Salavati-Niasari, J. Nanostruct. **5**, 169 (2015)
5. Z. Khayat Sarkar, F. Khayat Sarkar, Int. J. Nanosci. Nanotechnol. **7**, 197 (2011)
6. A. Ghasemi, A.M. Davarpanah, M. Ghadiri, Int. J. Nanosci. Nanotechnol. **8**, 207 (2012)
7. A. Rahdar, M. Aliahmad, Y. Azizi, J. Nanostruct. **5**, 145 (2015)
8. J. Safaei-Ghomi, S. Zahedi, M. Javid, M.A. Ghasemzadeh, J. Nanostruct. **5**, 153 (2015)
9. F.C.D. Lemos, E. Longo, E.R. Leite, D.M.A. Melo, A.O. Silva, J. Solid State Chem. **177**, 1542 (2004)
10. H. Fujisawa, M. Okaniwa, H. Nonomura, M. Shimizu, H. Niu, J. Eur. Ceram. Soc. **24**, 1641 (2004)
11. H. Nonomura, M. Nagata, H. Fujisawa, M. Shimizu, H. Niu, K. Honda, Appl. Phys. Lett. **86**, 163106 (2005)
12. S. Clemens, T. Schneller, R. Waser, A. Rudiger, F. Peter, S. Kronholz, T. Schmitz, S. Tiedke, Appl. Phys. Lett. **87**, 142904 (2005)
13. P.S. Pizani, E.R. Leite, F.M. Pontes, E.C. Paris, J.H. Rangel, E.J.H. Lee, E. Longo, P. Delega, J.A. Varela, Appl. Phys. Lett. **77**, 824 (2000)
14. G. Rosenman, D. Shur, Ya.E. Krasik, A. Dunaevsky, J. Appl. Phys. **88**, 6109 (2000)
15. G. Shirane, R. Pepinsky, Acta Crystallogr. **9**, 131 (1956)
16. S. Tang, Y. Deng, S.Z. Zhan, J. Thermal Anal. Calorimetry **104**, 653 (2011)
17. F.M. Pontes, J.H.G. Rangel, E.R. Leite, E. Longo, J.A. Varela, E.B. Araújo, J.A. Eiras, J. Mater. Sci. **36**, 3565 (2001)
18. R. Tickoo, R.P. Tandon, N.C. Mehra, P.N. Kotru, Sci. Eng. B **94**, 1 (2002)
19. J. Tartaj, C. Moure, P. Durán, Ceram. Int. **27**, 741 (2001)
20. J. Tartaj, J.F. Fernández, M.E. Villafuerte-Castrejón, Mater. Res. Bull. **36**, 479 (2001)
21. R. Sirera, M.L. Calzada, Mater. Res. Bull. **30**, 11 (1995)
22. D. Bersani, P.P. Lottici, A. Montenero, S. Pigoni, G. Gnappi, J. Non-Cryst. Solids **490**, 192 (1995)
23. M.L. Calzada, L. DelOlmo, J. Non-Cryst. Solids **121**, 413 (1990)
24. K. Ishikawa, N. Okada, K. Takada, T. Nomura, T. Hagino, J. Appl. Phys. **33**, 3495 (1994)
25. A. Safari, Y.H. Lee, A. Halliyal, R.E. Newnham, Am. Ceram. Soc. Bull. **66**, 668 (1987)
26. C.E. Millar, L. Pedersen, W.W. Wolny, Ferroelectrics **133**, 271 (1992)
27. K. Hirakata, W.E. Rhine, M.J. Cima, Am. Ceram. Soc. **79**, 1002 (1996)
28. M. Riazian, J. Nanostruct. **4**, 433 (2014)